Mesoscopic nanoshells: Geometry-dependent plasmon resonances beyond the quasistatic limit

Felicia Tam
Department of Physics and Astronomy, Rice University, Houston, Texas 77005, USA and Laboratory for Nanophotonics, Rice University, Houston, Texas 77005, USA

Allen L. Chen
Laboratory for Nanophotonics, Rice University, Houston, Texas 77005, USA

Janardan Kundu and Hui Wang
Laboratory for Nanophotonics, Rice University, Houston, Texas 77005, USA and Department of Chemistry, Rice University, Houston, Texas 77005, USA

Naomi J. Halas[a)]
Laboratory for Nanophotonics, Rice University, Houston, Texas 77005, USA, Department of Chemistry, Rice University, Houston, Texas 77005, USA, and Department of Electrical and Computer Engineering, Rice University, Houston, Texas 77005, USA

(Received 19 June 2007; accepted 17 September 2007; published online 27 November 2007)

The plasmon response of a spherical metallic shell becomes significantly more complex as its size is increased beyond the quasistatic limit. With increasing size and decreasing aspect ratio (r_1/r_2), higher order multipolar modes contribute in a more dominant manner, and two distinct core-shell geometries exist that provide the same dipole plasmon resonance, with differing relative multipolar contributions in their overall spectral response. With further increase in particle size, the geometric tunability of the core-shell structure disappears, and in the infinite radius limit the plasmon response is consistent with that of a thin metallic film. © *2007 American Institute of Physics*.
[DOI: 10.1063/1.2796169]

INTRODUCTION

In recent years, metallic nanoparticles and nanostructures have generated an immense amount of scientific and technological interest due to the unique characteristics of their interaction with light. The collective electronic, or plasmon, resonances of metallic nanostructures provide the mechanism for this strong interaction. In certain metallic nanostructures, the plasmon resonance frequency can be highly dependent on the shape of the nanostructure. For example, in a hollow metallic sphere with a dielectric core, known as a nanoshell, the plasmon frequency quite sensitively depends on the relative size of the inner and outer radii of the shell layer of the nanostructure.[1–3] The plasmon response of metallic shell particles has been shown to be remarkably robust in the presence of defects or imperfections in the nanoparticle's metallic layer.[4]

It has recently been shown that plasmons in metallic nanostructures interact in a manner analogous to the hybridization of wave functions of simple atoms and molecules.[5,6] The plasmon hybridization picture provides an underlying theoretical understanding of the geometry-dependent resonant properties of metallic nanostructures of various shapes, as well as the resonant properties of nanoparticle aggregates.[7] Because of this, metallic nanostructures can also be considered "artifical molecules," whose plasmon energies are determined in analogy with molecular orbital theory, while their properties can also be calculated more conveniently by applying electromagnetic theory. The plasmonic properties of nanoshells can be understood most straightforwardly in the quasistatic limit, where the size of the nanoshell is much smaller than the spatial wavelength of light whose frequency corresponds to its (bonding) plasmon resonance. However, as the dimensions of the core-shell nanoparticle are increased beyond the quasistatic limit, the properties of the plasmons supported by this structure become dependent on the overall size of the particle. Known as phase retardation (or finite size) effects, the immediate impact of increasing particle size beyond the quasistatic limit results in a systematic shifting of the dipole plasmon to slightly lower energies and a significant broadening of the plasmon resonance linewidth.[8,9] Higher order multipolar resonances appear as particle size is increased, as distinct spectral features at energies higher than that of the dipolar plasmon energy. Nanoshell-based plasmonic structures such as the dielectric-metal-dielectric-metal layered spherical nanoparticle or "nano-matryushka,"[5,10] also manifest finite size effects, seen in the asymmetric splitting of their hybridized plasmon resonances relative to the energies of the parent plasmons. While these systems show the effects of increasing particle size beyond the quasistatic regime, modifications of the plasmon resonance as particle size is increased still further have not yet been examined.

In this study we examine the changes to the Au nanoshell plasmon response as the particle size is increased far beyond the quasistatic limit. Mie scattering theory with

[a)]Electronic mail: halas@rice.edu

the empirically obtained dielectric function for Au[11] is utilized to calculate the wavelengths of the plasmon resonances for particles of increasing particle diameter. Changes in the plasmon energies and line shapes as a function of particle size and internal geometry are investigated. Nanoshells in this larger size range are fabricated by adapting fabrication methods developed earlier for nanoshells in the quasistatic regime, to compare theoretical predictions with experimentally observed optical extinction spectra for mesoscopic nanoshells with plasmon resonances in the midinfrard spectral range.

EXPERIMENTAL

Tetraethyl orthosilicate (TEOS 99.9999%), (3-aminopropyl) triethoxysilane (APTES), tetrachoroauric acid, *n*-dodecanethiol, and poly(4-vinylpyridine) (160 000 MW) were purchased from Sigma-Aldrich (St. Louis, MO) and used as received. Ammonium hydroxide, ethanol, and chloroform were obtained from Fisher Scientific (Hampton, NH). Ultrapure water (18.2 MΩ resistivity) was obtained from a Milli-Q water purification system (Millipore, Billerica, MA). Particle sizes were measured using scanning electron microscope images from either a JEOL 6500 scanning electron microscope or a FEI XL-30 environmental scanning electron microscope. Characterization of the optical extinction of the nanoshells was achieved using a Varian Cary 5000 UV-vis-NIR spectrometer and a Nicolet Magna-IR 560.

Au-silica nanoshells were fabricated based on a method previously described.[2,12] Briefly, silica nanoparticles 150–350 nm in radii were fabricated via the Stöber method,[13,14] and functionalized with APTES. The amine moiety of APTES serves to bind small (<5 nm in diameter) gold colloid[15] to the silica surface. A complete gold shell was grown onto the decorated silica surface by $HAuCl_4$ reduction in the presence of formaldehyde.

Extinction measurements were carried out with nanoshells either suspended in choloroform or immobilized on a silicon wafer. To promote nanoshell stability in chloroform, the nanoshell solution was mixed with a 110 mg/ml (aq) solution of poly(vinylpyrrolidone) (40 000 MW, PVP-40).[16] The amount of PVP-40 solution to add was calculated to provide 60 PVP-40 molecules per nm^2 of nanoparticle surface area. Excess PVP-40 was removed through multiple cycles of centrifugation and resuspension in water and then ethanol. Likewise, transfer to chloroform was achieved through 3 cycles of centrifugation and resuspension in chloroform.

The largest nanoshells studied were characterized optically while immobilized on silicon substrates. A well-dispersed, submonolayer of nanoshells was deposited onto a silicon wafer in a process described previously[17,18] in which poly(4-vinylpyrridine) was adsorbed onto the silicon wafers to act as an adhesion layer for nanoshell deposition. This substrate is then immersed in an aqueous suspension of nanoshells, and then rinsed with ethanol and dried with a stream of dry N_2.

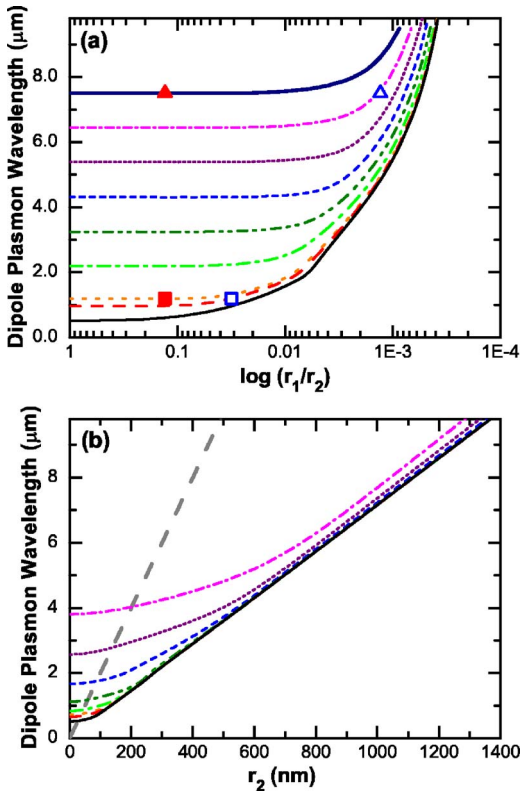

FIG. 1. (Color online) Size-dependent nanoshell plasmon resonances. Calculated dipole plasmon resonance of silica-core gold-shell nanoshells in a homogeneous dielectric environment of water (a) as a function of aspect ratio r_1/r_2 with overall radii r_2 of 1 (solid), 129 (dashed), 162 (dotted), 300 (dash dotted), 450 (dash dot dotted), 600 (short dashed), 752 (short dotted), 900 (short dash dotted), and 1047 nm (thick solid). (■, □, ▲, △) correspond to spectra plotted in Fig. 2. (b) The dipole plasmon resonance as a function of r_2 for aspect ratios of 0.995 (short dash dotted), 0.99 (short dotted), 0.98 (short dashed), 0.95 (dash dot dotted), 0.90 (dash dotted), 0.85 (dotted), 0.8 (dashed), and 0 (solid, solid nanosphere). Particle diameters smaller than λ/10 (thick dashed gray line) correspond to the plasmon hybridization regime and those larger than λ/10 correspond to the phase retardation regime.

RESULTS AND DISCUSSION

In the electrostatic limit, the plasmon energies of a nanoshell depend only on their aspect ratio r_1/r_2. In Fig. 1(a), the bonding dipole plasmon resonance energy of silica core-Au shell nanoshell particles in water is calculated using Mie scattering theory as a function of aspect ratio r_1/r_2 for a discrete number of outer radii ranging from $r_2=1$ to 1047 nm. For the smallest particle size considered, $r_2=1$ nm, the nanoshell remains well within the quasistatic limit, corresponding to the results of earlier studies.[2] From the plasmon hybridization model, the strong redshift of the plasmon resonance as $r_1/r_2 \rightarrow 1$ $[\log(r_1/r_2) \rightarrow 0]$ can be understood as an increase in the interaction of the sphere and cavity plasmons supported by the nanoshell geometry.[5,6] With decreasing aspect ratio, this interaction becomes weaker and the observable bonding nanoshell plasmon resonance approaches the plasmon resonance of a solid Au nanosphere, at 520 nm. The sphere resonance represents the low wavelength limit of the nanoshell dipole plasmon resonance. As the total particle size is increased, the resonant wavelength of the nanoshell plasmon begins to depart from the

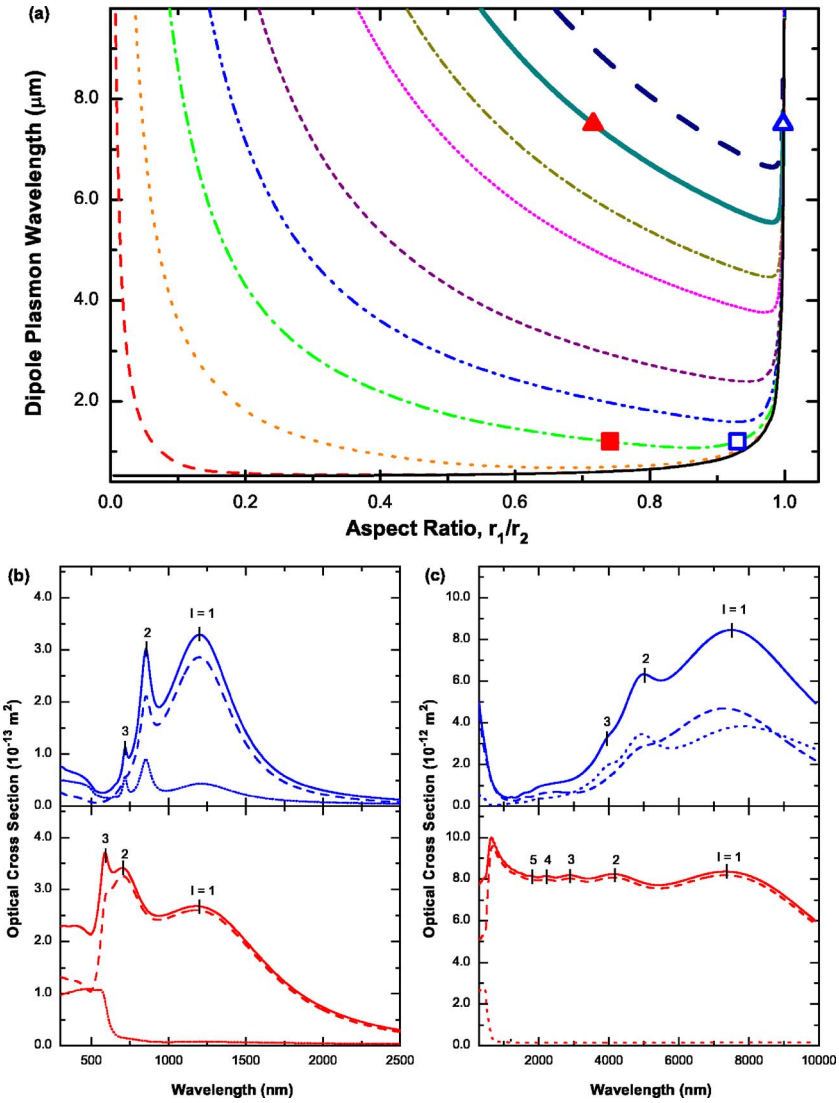

FIG. 2. (Color online) (a) Calculated dipole plasmon resonance of silica-core gold-shell nanoshells with core radii of 0.1 (solid), 10 (dashed), 50 (dotted), 120 (dash dotted), 200 (dash dot dotted), 300 (short dashed), 500 (short dotted), 600 (short dash dotted), 750 (thick solid), and 900 nm (thick dashed navy). Representative spectra are plotted in (b) (□, ■) and in (c) (△, ▲). (b) Extinction (solid), scattering (dashed), and absorption (dotted) cross sections for nanoshells with r_1 =120 nm and a dipole plasmon resonance at 1200 nm. The marked multipole plasmon modes with l =1,2,3,… correspond to the dipole, quadrupole, octupole, … modes, respectively. (c) Same as (b) for two nanoshells with r_1=750 nm and a dipole resonance at 7500 nm. The multipole modes with $l>5$ in the spectra of the nanoshell with the thicker shell overlap, forming a broad continuum at shorter wavelengths.

trend observed in the quasistatic regime. In particular, low aspect ratio nanoshells possess longer wavelength resonances than they would for the same aspect ratio in the quasistatic regime. As the overall particle size is increased, the electromagnetic field of incident light at resonance is no longer uniform over the entire particle, resulting in the excitation of higher order plasmon modes and a redshifting of the dipolar plasmon.[8,19] However, for these larger nanoshell sizes the strong redshift of the plasmon resonance with increasing aspect ratio results in an expansion of the electrostatic limit to larger aspect ratios, as seen in the shape changes in the curves coalescing as $r_1/r_2 \rightarrow 1$.

The size-dependent plasmon response can also be examined by plotting the dipole plasmon resonance of a nanoshell as a function of overall particle size [Fig. 1(b)]. For r_2 $<$50 nm, each aspect ratio yields a distinct plasmon energy. This is the electrostatic regime, where the plasmon resonances are independent of nanoparticle size. As the particle size increases, the dipole plasmon resonance begins to increase in wavelength, indicating the onset of phase retardation effects. This size-dependent redshifting of the plasmon energy is more pronounced for particles with shorter wavelength plasmons. Traditionally, the quastistatic limit is defined by particle sizes less than $\lambda/10$. Therefore, particles with the shortest wavelength plasmons are the first to experience phase retardation effects as their total size is increased. In fact, it is evident that the nanoshell plasmons begin to redshift from phase retardation effects even when the particle diameter $2r_2$ is less than $\lambda/10$. As the particle size is increased and phase retardation effects become dominant, all dipole plasmons shift to higher wavelength. For sufficiently large r_2, the optical properties of the particles become completely independent of r_1; in other words, the plasmon response is due only to the plasmon on the outer surface of the particle. As r_2 increases further, the plasmon wavelength increases linearly with particle size, with a slope of ~7.1. This large particle limit is consistent with the lowest energy state of a thin film plasmon, which also approaches infinite wavelength corresponding to zero energy.[21] A metal film can support a continuum of plasmon energies ranging from the resonant surface plasmon frequency to zero, and an increasingly large nanoshell supports an increasing number of multipolar modes. In the limit of infinite nanoparticle size, the nanoshell plasmon is equivalent to that of a thin film; conversely, a thin film can also be conceived of as an infinite radius nanoshell.

In order to guide experimental fabrication of nanoshells at a desired plasmon resonance wavelength, it is useful to understand the resonant behavior of nanoshells with a given inner radius and various aspect ratios, corresponding to different shell thicknesses [Fig. 2(a)]. As expected, for $r_1 = 0.1$ nm, well within the quasistatic regime, the dipole plasmon wavelength decreases with decreasing aspect ratio, to a lower wavelength limit of 520 nm, corresponding to the plasmon resonance of a solid nanosphere. Nanoshells with high aspect ratios for all the core radii investigated are also within the quasistatic regime, and follow the behavior of the $r_1 = 0.1$ nm curve as $r_1/r_2 \rightarrow 1$. However, as the aspect ratio decreases, the overall particle size is increased, and this trend no longer applies. In the phase retardation regime, the plasmon resonance shifts to longer wavelengths as the aspect ratio decreases. The aspect ratio at which this change in behavior occurs increases as the core radius is increased. Thus, when the particle size is beyond the quasistatic limit, two differing values of aspect ratio for each core size support a dipolar plasmon response at the same wavelength. Characteristic extinction spectra for these two solutions are shown in Figs. 2(b) and 2(c), for two different core radii of 120 and 750 nm. In these spectra, a pronounced difference can be seen in the overall plasmon spectral response for each particle, with far more multipolar contributions arising in the spectra of the thicker shell particles. As particle size is increased still further, the overall geometric tunability of the nanoshell structure is decreased, and phase retardation becomes a more dominant factor determining the plasmon resonance of the nanoshell. For small aspect ratios, a solution that converges to a solid metallic sphere plasmon response when $r_1/r_2 \rightarrow 0$, the size dependence of the plasmon resonance is most pronounced. This corresponds to the redshifts in plasmon resonance wavelength, a "tunability" that is due solely to phase retardation effects, which is observed for solid metallic nanospheres of increasing particle size.

It has previously been suggested that the tuning range of a Au-silica nanoshell is reduced when the scattering cross section becomes significant.[20] This finding is consistent with our study, which also shows that an increase in scattering cross section relative to absorption cross section at the dipole plasmon resonance occurs when the particle is just larger than the quasistatic regime [Figs. 2(b) and 2(c)]. However, these authors also conclude that it would be undesirable to fabricate nanoshells with large core sizes because the nanoshells would inherently scatter more and have limited tunability. The spectrum of the larger core-shell ratio nanoshell in Fig. 2(c) shows that this is not necessarily the case. The scattering and absorption cross sections for this nanoshell are comparable; so here scattering has yet to become predominant, even though the core is larger than a micron in diameter. Therefore, we find that it is indeed possible and advantageous to tune nanoshells to the mid-IR by increasing nanoparticle size in addition to manipulating the core-shell ratio.

In order to verify that our calculations are valid for larger particles in the phase retardation regime, the experimental spectra of mid-IR nanoshells were compared with theoretical spectra. For these measurements the particles were dispersed in chloroform as a solvent, to minimize the presence of infrared absorption bands typical of other commonly used solvents. The theoretical extinction efficiency of nanoshells was determined using particle dimensions measured via electron microscopy and with a uniform dielectric environment of chloroform ($n = 1.44$). In Fig. 3, it can be seen that the experimental and theoretical spectra agree quite well. Mie theory allows us to decompose the nanoshell spectra into its individual multipolar components. Figure 3(a) shows the experimental and theoretical spectra for a $[r_1, r_2] = [217, 234]$ nm nanoshell. Four multipole plasmon modes are discernable in this spectrum. The corresponding spectrum for a larger nanoshell, $[r_1, r_2] = [360, 372]$ nm [Fig. 3(b)], shows that five multipole modes are present in this experimental spectrum, where we observe that more multipoles are evident for larger particles, as expected.

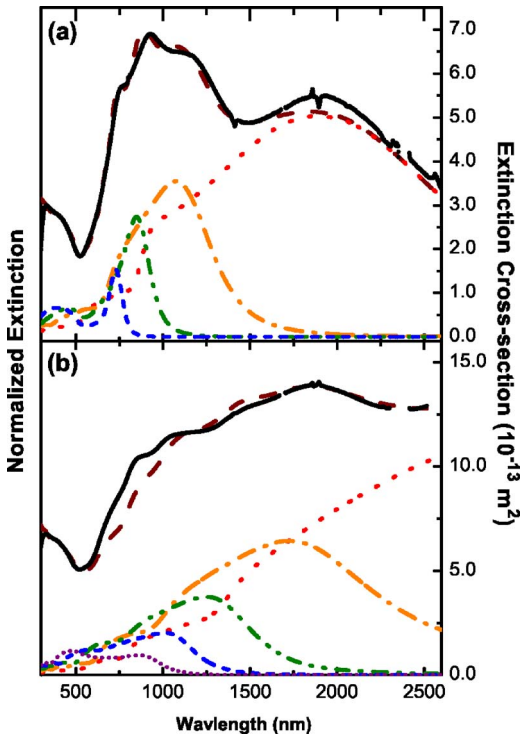

FIG. 3. (Color online) Experimental (solid, left axis) and theoretical (dashed, right axis) extinction spectra for two nanoshells in chloroform suspension. (a) Nanoshell with $[r_1, r_2] = [217, 234]$ nm. (b) Nanoshell with $[r_1, r_2] = [360, 372]$ nm. The calculated spectra are deconvolved into the various multipole modes: $l = 1$ (dotted), 2 (dash dotted), 3 (dash dot dotted), 4 (short dashed), and 5 (short dotted).

In order to study silica core-Au shell particles in the micron size regime, we fabricated nanoshells with $[r_1, r_2] = [482, 510]$ nm [Fig. 4(a)]. Such large sized metallized particles are highly prone to solution-phase aggregation due to large interparticle van der Waals interactions. As a result, the micron-sized particles were dispersed on silicon substrates prior to optical characterization to avoid aggregation, which dramatically modifies the plasmon response of nanoshells, introducing dimer plasmon modes at longer wavelengths.[22] Silicon provides high transparency in the spectral range of $1-10$ μm.

The extinction spectrum of the micron-sized particles [Fig. 4(b)] shows the multimodal plasmon response of the

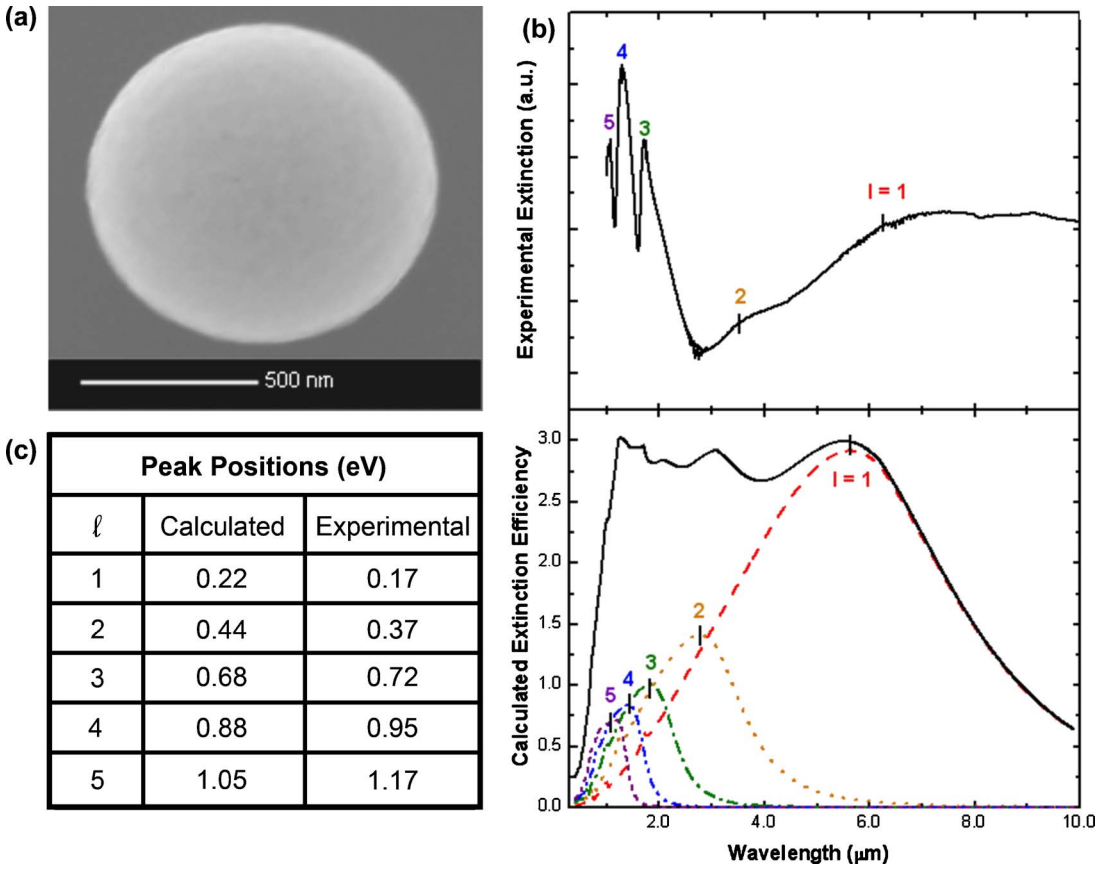

(c)

Peak Positions (eV)		
ℓ	Calculated	Experimental
1	0.22	0.17
2	0.44	0.37
3	0.68	0.72
4	0.88	0.95
5	1.05	1.17

FIG. 4. (Color online) Experimental and theoretical spectra of mid-IR nanoshells on a silicon substrate. (a) scanning electron microscopy micrograph of a mid-IR resonant nanoshell with $[r_1, r_2]=[482, 510]$ nm. (b) Experimental (upper) extinction spectra and calculated (lower) extinction efficiency for the nanoshell embedded in a weighted average of the dielectric constants of silicon and air, allowing us to assign the multipole peaks in the experimental spectrum. (c) Comparison of the spectral locations of the experimental and calculated peaks.

nanoshells ranging from visible to mid-IR energies. Due to the inhomogeneous environment of the particles, direct comparison with Mie scattering theory calculations is only qualitative in this case. However, for comparative purposes, an effective dielectric embedding medium of $\varepsilon=3.48$ was determined, corresponding to a weighted average of the dielectric constants of the component media[23] (80% air and 20% Si). Under this assumption, the experimental and theoretical plasmon resonance energies can be compared [Fig. 4(b)].[24]

In comparing the experimental and calculated spectra [Fig. 4(c)], the multipole plasmon resonance spectral features appear significantly more distinct in the experimental spectrum than theory. This may be attributable to the local anisotropic environment of the particles used in the experiment which is not captured by our theoretical approach, and merits further study. The overlap of the fringing field of the micron-sized particles with the silicon substrate may give rise to the modifications in the multipolar plasmon response of the particles that are observed. In addition, particles in this size regime are capable of supporting whispering gallery modes which may contribute to their optical response and may also be enhanced by the refractive substrate. Despite these discrepancies, qualitative agreement between Mie scattering theory with an effective medium and the experimentally observed plasmon response is sufficient for predicting the plasmon response of particles in this large size regime.

In conclusion, we have examined the effect of increasing particle size of a metallic shell particle from the quasistatic limit to the micron size range, where phase retardation effects become very important in the particle's plasmon response. We have shown that Mie scattering theory can quantitatively predict the plasmon response of large mid-IR nanoshells in a homogeneous dielectric environment and can also accurately model the behavior of the complex multipolar plasmon resonances observable in mesoscopic nanoshells.

ACKNOWLEDGMENTS

The authors would like to thank Peter Nordlander for insightful discussions on this subject. This work is supported by Air Force Office of Scientific Research Grant No. F49620-03-C-0068, National Science Foundation (NSF) Grant Nos. EEC-0304097 and ECS-0421108, the Texas Institute for Bio-Nano Materials and Structures for Aerospace Vehicles funded by NASA Cooperative Agreement No. NCC-1-02038, the Robert A. Welch Foundation Grant No. C-1220, and the Multidisciplinary University Research Initiative (MURI) Grant No. W911NF-04-01-0203.

[1] R. D. Averitt, D. Sarkar, and N. J. Halas, Phys. Rev. Lett. **78**, 4217 (1997).
[2] S. J. Oldenburg, R. D. Averitt, S. L. Westcott *et al.*, Chem. Phys. Lett. **288**, 243 (1998).
[3] E. Prodan and P. Nordlander, Nano Lett. **3**, 543 (2003).
[4] C. Oubre and P. Nordlander, J. Phys. Chem. B **108**, 17740 (2004).
[5] E. Prodan, C. Radloff, N. J. Halas *et al.*, Science **302**, 419 (2003).

[6] E. Prodan and P. Nordlander, J. Chem. Phys. **120**, 5444 (2004).
[7] H. Wang, D. Brandl, P. Nordlander *et al.*, Acc. Chem. Res. **40**, 53 (2007).
[8] S. J. Oldenburg, G. D. Hale, J. B. Jackson *et al.*, Appl. Phys. Lett. **75**, 1063 (1999).
[9] S. L. Westcott and N. J. Halas, Phys. Rev. B **66**, 155431 (2002).
[10] C. Radloff and N. J. Halas, Nano Lett. **4**, 1323 (2004).
[11] P. B. Johnson and R. W. Christy, Phys. Rev. B **6**, 4370 (1972).
[12] S. J. Oldenburg, S. L. Westcott, R. D. Averitt *et al.*, J. Chem. Phys. **111**, 4729 (1999).
[13] W. Stober, A. Fink, and E. Bohn, J. Colloid Interface Sci. **26**, 62 (1968).
[14] W. Wang, B. H. Gu, L. Y. Liang *et al.*, J. Phys. Chem. B **107**, 12113 (2003).
[15] D. G. Duff, A. Baiker, and P. P. Edwards, Langmuir **9**, 2301 (1993).
[16] C. Graf, D. L. J. Vossen, A. Imhof *et al.*, Langmuir **19**, 6693 (2003).
[17] S. Malynych, I. Luzinov, and G. Chumanov, J. Phys. Chem. B **106**, 1280 (2002).
[18] F. Tam, C. Moran, and N. Halas, J. Phys. Chem. B **108**, 17290 (2004).
[19] S. L. Westcott, J. B. Jackson, C. Radloff *et al.*, Phys. Rev. B **66**, 155431 (2002).
[20] S. Schelm and G. B. Smith, J. Opt. Soc. Am. A Opt. Image Sci. Vis **22**, 1288 (2005).
[21] H. R. Raether, *Surface Plasmons on Smooth and Rough Surfaces and on Gratings* (Springer-Verlag, New York, 1988).
[22] D. W. Brandl, C. Oubre, and P. Nordlander, J. Chem. Phys. **123**, 024701 (2005).
[23] M. D. Malinsky, K. L. Kelly, G. C. Schatz *et al.*, J. Phys. Chem. B **105**, 2343 (2001).
[24] E. Prodan, A. Lee, and P. Nordlander, Chem. Phys. Lett. **360**, 325 (2002).